

Image Quality Improvement in Kidney Stone Detection on Computed Tomography Images

Saman Ebrahimi and Vladimir Y. Mariano

Institute of Computer Science, University of the Philippines Los Baños, Laguna, Philippines

Email: saman.ibrahimi1364@gmail.com, vymariano@up.edu.ph

Abstract—Kidney-Urine-Belly computed tomography (KUB CT) analysis is an imaging modality that has the potential to enhance kidney stone screening and diagnosis. This study explored the development of a semi-automated program that used image processing techniques and geometry principles to define the boundary, and segmentation of the kidney area, and to enhance kidney stone detection. It marked detected kidney stones and provided an output that identifies the size and location of the kidney based on pixel count. The program was tested on standard KUB CT scan slides from 39 patients at Imam Reza Hospital in Iran who were divided into two groups based on the presence and absence of kidney stones in their hospital records. Of these, the program generated six inconsistent results which were attributed to the poor quality of the original CT scans. Results showed that the program has 84.61 per cent accuracy, which suggests the program's potential in diagnostic efficiency for kidney stone detection.

Index Terms—renal calculi, kidney stones, computed tomography, image processing

I. INTRODUCTION

Renal calculus, more commonly known as kidney stone formation, is characterized by the formation of crystals in the urine caused by substance concentration or genetic susceptibility. All persons are susceptible to kidney stones, even infants, and yet, the majority of kidney stone cases remain undetected except in cases where extreme abdominal pain is exhibited or abnormal urine color is observed. In addition, people with kidney stones exhibit common signs such as fever, pain and nausea that are easily associated to other conditions. Kidney stone detection is important particularly in its early stages to facilitate intervention or to receive proper medical treatment. The presence or the recurring presence of kidney stone decreases kidney functions and dilation of the kidney. It also has implications on the degrees of chronic kidney disease (CKD) or chronic renal failure (CRF) for people who have not been previously diagnosed with this condition. However, because of its asymptomatic nature, it is commonly diagnosed among patients who undergo medical examination for other diseases such as cardiovascular diseases (CVD), diabetes, and other medical conditions predispose to the urogenital apparatus [1]-[3]. Today, computer-assisted tools such as

ultrasound imaging, computed tomography (CT), and X-rays that use intravenous pyelogram (IVP) provide the most accurate diagnostic tools for kidney stone screening and diagnosis. CT scans, which provide three-dimensional views of the organ or region of interest is the most sought after kidney stone screening tool in hospitals. Its convenience and efficiency in kidney stone detection (including its pathology) for both asymptomatic and symptomatic patients make advances in CT technology extremely important for physicians and patients alike [4], [5]. Software programming, which has found current and potential applications in technological advancements in the field of medicine, recognizes the need to contribute to CT screening development particularly in enhancing diagnosis of the kidney-urine-belly (KUB) region for kidney stone detection. This study developed a semi-automatic kidney screening program that integrated digital image processing and image analysis techniques in KUB CT images. Specifically, the study (1) developed a method for defining the boundary of regions of interest in a digital KUB CT scan; (2) developed a method for segmenting the region and object of interest in a digital KUB CT scan; and, (3) developed a method for detecting the object of interest (kidney stones) including its size and location in a digital KUB CT scan images. Fig. 1 shows the cross-section of abdomen.

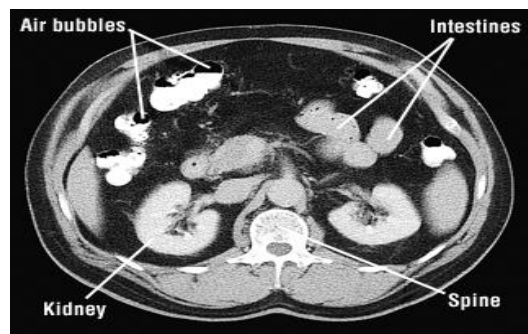


Figure 1. Cross-Section view of the abdomen

II. METHODOLOGY

The digitized transverse abdomen CT scan images were taken with Toshiba Aquilion 16 Slice CT scanner, and obtained from the Imam Reza Hospital in Iran (kums.ac.ir) through their Picture Archiving and Communication System (PACS). KUB CT scans from 39 patients with symptomatic and asymptomatic kidney

stone cases in 2014 were provided by the Imam Reza Hospital as subjects for the program prototype application. Each patient has 40 to 48 slices; of these, 10 patients were diagnosed without kidney stones, while the remaining 29 patients were diagnosed with variable kidney stone conditions through their CT scans by the hospital. This is to establish the degree of accuracy and efficiency of the program in distinguishing kidney stone cases which may be authenticated by a specialist. The program design was grounded on the application of image processing techniques and geometry principles. Image processing techniques applied in the program include Contrast Adjustment (Gamma Adjustment) [6], Segmentation [7]-[10], Binarization (Thresholding) [7], [11], [12], morphological operation [13]-[15], localization [14], Boolean operation [7], [11] and connected component [14], [15], while geometry principles and axioms were used to compute for distances between pixel points and center of mass [16]. These were used integratively in the program to develop six levels of image analyses (localization, contrast adjustment, segmentation, combining [17], connected component labeling [18], and restriction and object detection [19] to enhance kidney stone detection. The following procedures were undertaken: Using the KUB CT scans provided by the Imam Reza Hospital, the program analyzed slices from each patient where the kidney, the region of interest, is only visible. Since not all slices provide a clear view of the kidney, reading of slices begin at Slice 1, however analysis is read and merged where the kidney is visible such as shown in Fig. 2.

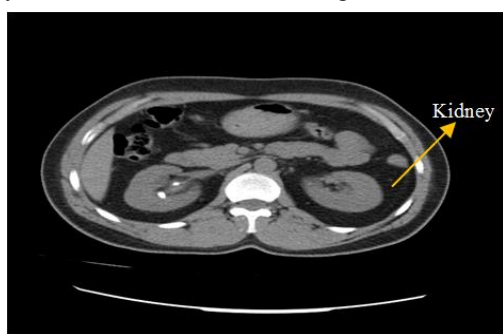


Figure 2. Sample of a KUB CT scan slice

A. Localization (Bounding Box)

Localization, which involves several steps, was applied to slices where the kidney is visible to focus on the abdomen, as the region of interest. Scanned images generally include extra parts around abdomen, and a bounding box is used to establish the area of interest (Fig. 3). Binarization was applied in each slice using thresholding equal to 10 before application to the bounding box in the KUB region. This allows segmentation of the foreground (abdomen) by a white color and the background by a black color. Morphological operation such as dilation and erosion were applied respectively to isolate the object of interest (abdomen) in the foreground. This allows detection of the connected component through application of the 8-connection connectivity which identifies any component

pixel equal to 1 in the foreground. All pixels that equal to 1 are connected; if a pixel is equal to 0 a boundary of the connected component will be established. To overcome computation of distances around the abdomen when applying connected component, the program establishes a bounding box from individual computation of the distance from the topmost and bottommost pixel (height), and the rightmost and leftmost pixel (width) of the abdomen to generate two horizontal and vertical lines that will enclose the area.

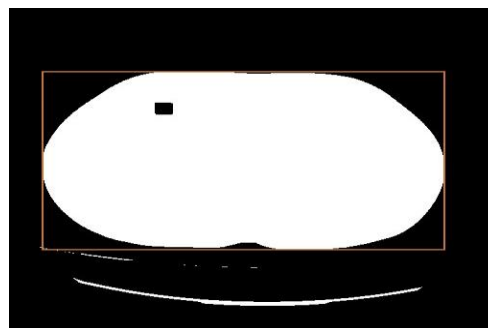


Figure 3. Result of the bounding box in the abdomen area when applied to a slice.

B. Contrast Adjustment (Gamma Adjustment)

This level is exploratory in nature and was the program's foundation in applying threshold in image processing. It employed application of gamma adjustment

$$F(x) = X^a \quad (1)$$

As a refining method prior to application of thresholding to allow further image adjustment options. All gamma adjustments were done in the range of 1 to 3.5 by step 0.1 (1.1, 1.2, 1.3... 3.4, 3.5) before application of thresholding in each adjustment. Thresholding established the optimum value for gamma adjustment ($gamma = 2.5$); values greater than 2.5 result to data loss in some slices, i.e., the objects (stones) tend to disappear after thresholding, while values less than 2.5 failed to diminish unwanted objects even after thresholding (Fig. 4).



Figure 4. Result of gamma 2.5 after its application to a slice.

C. Segmentation (Thresholding)

Thresholding is applied on the image resulting from gamma adjustment ($gamma = 2.5$) to allow segmentation of image the foreground (stone and bones) and background. The optimum threshold value for standard KUB CT images such as the ones used in this study is

intensity 120 (Fig. 5). When threshold values greater than 120 is applied, it will render the small stones inside the kidney to disappear, while values less than 120 will render some parts of the organs visible in the foreground. Pixels applied to threshold greater than 120 will appear in the foreground (white color), and threshold less than 120 was assigned to appear in the background.

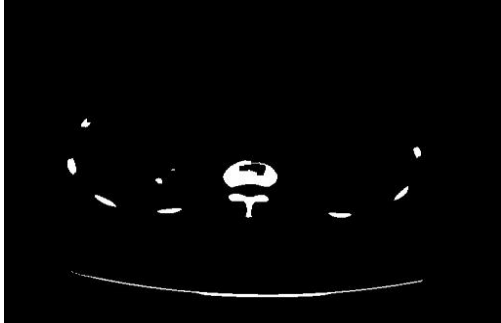


Figure 5. Result of threshold 120 after it was applied to a slice.

D. Combining the Slices Using Logical OR Operation

This level integrated all slices that were subjected to thresholding and organized in an array using the logical OR binary operation (Fig. 6). Beginning with the threshold result of the first slice (and moving progressively to the last slice), all pixels equal to 1 (foreground) were connected and a boundary established if the pixel in the image output is equal to 0 (background). All pixels equal to 1 are included in the output image.

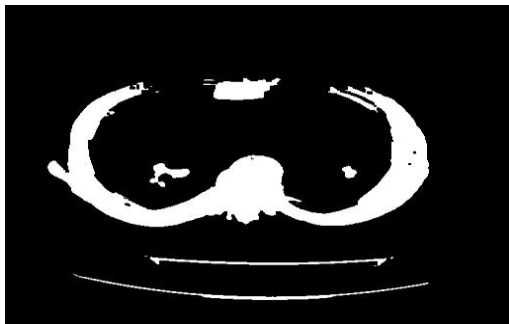


Figure 6. Combined slices generated from threshold application.

E. Connected Component Labeling

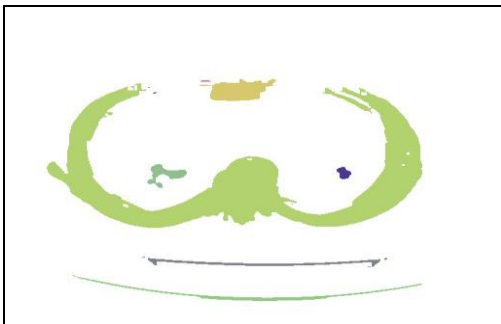


Figure 7. Application of connected component labeling to designate a color to each detected component.

This level detects all connected components inside the image resulting from combining the binary slices. This method functions by choosing a pixel that cross

references itself to 8 pixels surrounding it to determine if it has the same value as the center pixel and enabling it to become a part of the component. When applied to all pixels in the component, it determines differentiation by assigning a color to each detected component (Fig. 7).

F. Removing the Spine and Ribs

This level extracted the location of the spine based on the abdomen's boundary (torso bounding box), and then removed all pixels belonging to that connected component (spine and ribs). The spine's location was used as a guide to establish the point coordinates

$$X = width \div 2, Y = height \times 0.83 \quad (2)$$

In the abdomen compartment which determined that all pixels inside belong to the target component (spine and ribs). Fig. 8 shows the output after pixel conversion (pixel = white color) in the background. After using point coordinates to establish the abdomen boundary and locate the spine, the upper 30 percent of images were identified and its pixel values were converted to background since kidney stones are never detected in this region (Fig. 9).

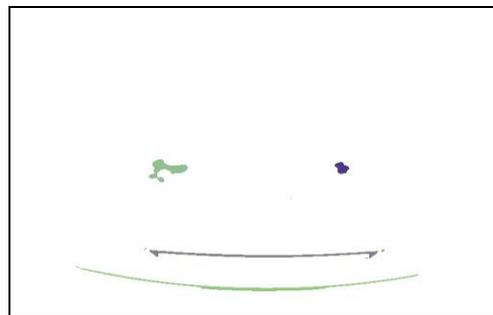


Figure 8. Image output after the conversion of pixels to white in the background which removed the spine.

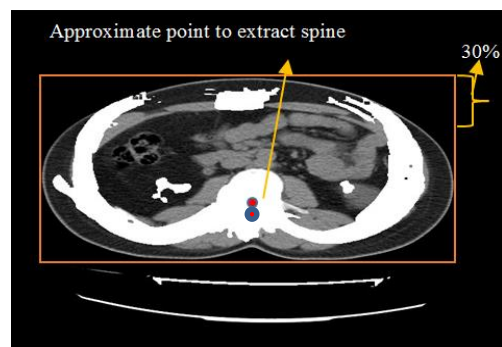


Figure 9. A point was used to detect the spine and mark the upper 30 percent of the image.

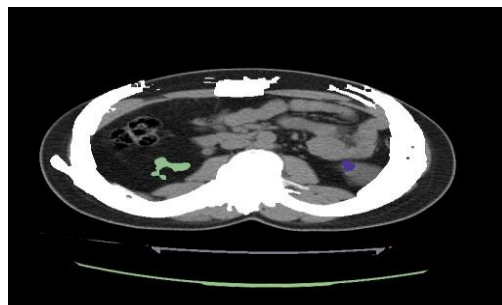


Figure 10. Aggregate image of the remainder component and the last slice

The colored component in the image was generated as output of the combined connected components resulting from the removal of the spine and ribs using the simple binary OR operation (Fig. 10).

G. Restriction and Object Detection

This level applied simple restriction to segment in the region of interest and to detect the target objects (kidney stones) inside. Arbitrary points (left and right) were selected and a distance formula was applied to create a virtual boundary to segment the region of interest. When the distance between the arbitrary point and the connected component is equal or less than computed distance, the component inside the segmented region is then shown in the output.

H. Virtual Region Segmentation

Established the location of the two arbitrary points from the abdomen bounding box left and right coordinates.

$$\begin{aligned} X.l &= torso.length \times 4 \div 10, Y.l = torso.depth \div 2 \\ X.r &= torso.length \times 4 \div 10, Y.r = torso.depth \div 2 \end{aligned} \quad (3)$$

The distance equivalent to 90 pixels was identified as a condition of focus for the connected component or the center of mass, and that objects with distances less than or equal this value from the arbitrary point shall be detected as target object. The virtual segmented region (enclosed in a circle) was established using said radius value relative to the center of mass (Fig. 11).

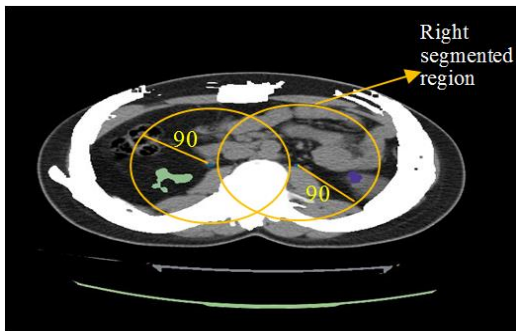


Figure 11. Segmented region inside virtual enclosures

I. Design Restriction to Segmented Region

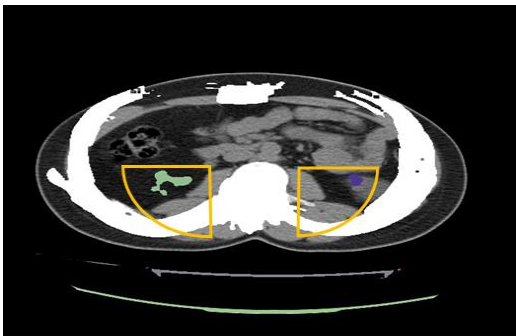


Figure 12. Restricted area in the segmented region

Since the segmented virtual region still cover a large section of unwanted component in the output, two virtual loops were drawn to enclose areas of interest in the image.

A restriction condition was designed to express control of the image (Fig. 12) using a center coordinate that specify command inclusion for the left kidney region ((*arbitrary.x* >= *component.x*) and (*arbitrary.y* <= *component.y*)), or the right kidney region ((*arbitrary.x* <= *component.x*) and (*arbitrary.y* <= *component.y*)).

J. Output

An image and text file was generated by the program as output. The image shows the algorithm detecting objects of interest in the left and right region of the kidney bound inside a box (Fig. 13), while the text file provided information such as the number of stones present inside each region, its specific location and its size (Fig. 14). The size of each stone was identified based on the number of pixels detected by the connected component labeling.

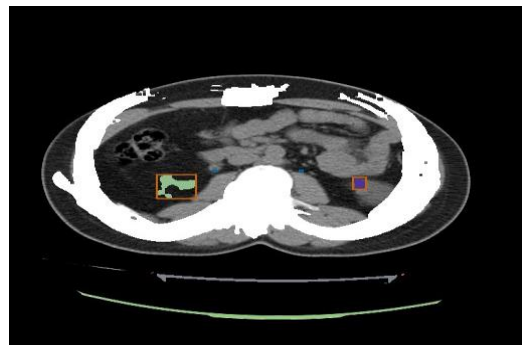


Figure 13. Sample output image.

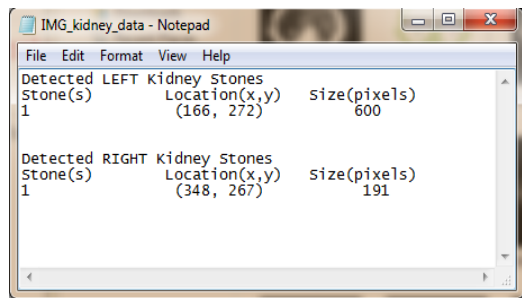


Figure 14. Sample text output file.

III. RESULTS AND DISCUSSION

A. Data Analysis and Prototype Application

Data analysis for this study was based on the incidence of kidney stone detected among patients. Results generated by the prototype program were cross-referenced with the patients' health records through their attending physician at Imam Reza Hospital to determine the degree of accuracy that the software lent in kidney stone detection.

B. Performance Evaluation

The results of the programs application among patients clinically diagnosed without kidney stones (Group 1) and patients clinically diagnosed kidney stones (Group 2) are shown in Table I and Table II, respectively. For Group 1 patients, the term CLEAN was used to indicate that the patient's hospital record shows no previous data of a

kidney stone. In reference to the output of the program, “NO” was used to indicate results that correspond to the patient’s hospital records (no kidney stone), and “YES” was used to indicate that the programs output is contrary to that.

TABLE I. CORRELATION OF PROGRAM OUTPUT AND HOSPITAL RECORD OF PATIENTS PREVIOUSLY DIAGNOSED WITHOUT KIDNEY STONES.

Patient Number	Recorded information in patient folder		Output of program	
	L-Kidney	R-Kidney	L-Kidney	R-Kidney
1	CLEAN	CLEAN	NO	NO
2	CLEAN	CLEAN	NO	NO
3	CLEAN	CLEAN	NO	NO
4	CLEAN	CLEAN	NO	YES
5	CLEAN	CLEAN	NO	NO
6	CLEAN	CLEAN	NO	NO
7	CLEAN	CLEAN	NO	NO
8	CLEAN	CLEAN	NO	NO
9	CLEAN	CLEAN	NO	NO
10	CLEAN	CLEAN	NO	NO

Results on Table I shows that program output correspond to hospital record files of the patients except one, Patient Number 4. The program provided an incorrect output for the patient due to the inaccurate KUB scan of the torso. The boundaries of the torso do not complement each other at all levels resulting to the detection of the spine as a stone (Fig. 15). An Recall formula was used to compute for the accurate output generated 90 percent efficiency.

$$Recall = (correct\ detected\ cases \times 100) \div (all\ cases) \quad (4)$$

$$Recall = (9 \times 100) \div (10) = 90$$

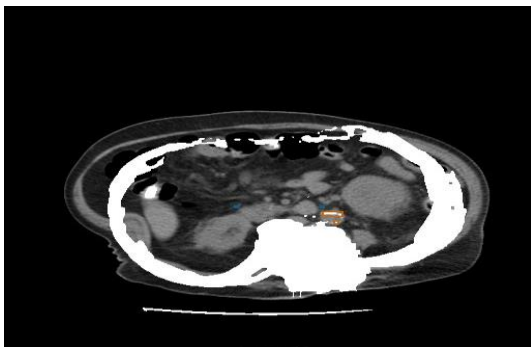


Figure 15. Sample of an incorrect program output which indicates that a patient has kidney stone when hospital records indicated otherwise

Table II shows the result of cross-referencing patient hospital records with program output of this study for Group 2 patients. The table uses “YES” to indicate that the program generated the same output as the patient’s hospital record (with kidney stones). “NO” was used in this table to indicate that the program output did not detect any kidney stones contrary to the patient’s hospital records (with kidney stone). Data shows that five (5) of the 29 patients have inconsistent results in the program. These are Patient Numbers 2, 3, 25, 26 and 27. Recall of program for this group is equal to:

$$Recall = (24 \times 100) \div (29) = 82.75$$

TABLE II. CORRELATION OF PROGRAM OUTPUT AND HOSPITAL RECORD OF PATIENTS PREVIOUSLY DIAGNOSED WITH KIDNEY STONES.

Patient Number	Recorded information in patient folder		Output of program	
	L-Kidney	R-Kidney	L-Kidney	R-Kidney
1	2 STONES	1 STONE	YES	YES
2	2 STONES	2 STONES	NO	NO
3	CLEAN	2 STONES	YES	NO
4	3 STONES	CLEAN	YES	YES
5	4 STONES	CLEAN	YES	YES
6	1 STONE	CLEAN	YES	YES
7	1 STONE	CLEAN	YES	YES
8	CLEAN	3 STONES	YES	YES
9	1 STONE	2 STONES	YES	YES
10	1 STONE	1 STONE	YES	YES
11	SOME	SOME	YES	YES
12	1 STONE	2 STONES	YES	YES
13	2 STONES	1 STONE	YES	YES
14	SOME	SOME	YES	YES
15	1 STONE	CLEAN	YES	YES
16	CLEAN	1 STONE	YES	YES
17	SOME	CLEAN	YES	YES
18	2 STONES	CLEAN	YES	YES
19	4 STONES	CLEAN	YES	YES
20	3 STONES	CLEAN	YES	YES
21	SOME	1 STONE	YES	YES
22	2 STONES	1 STONE	YES	YES
23	CLEAN	2 STONES	YES	YES
24	CLEAN	1 STONE	YES	YES
25	CLEAN	1 STONE	YES	NO
26	1 STONE	CLEAN	NO	YES
27	CLEAN	SOME	YES	NO
28	CLEAN	1 STONE	YES	YES
29	3 STONES	CLEAN	YES	YES

For Patient Number 2, (Fig. 16).

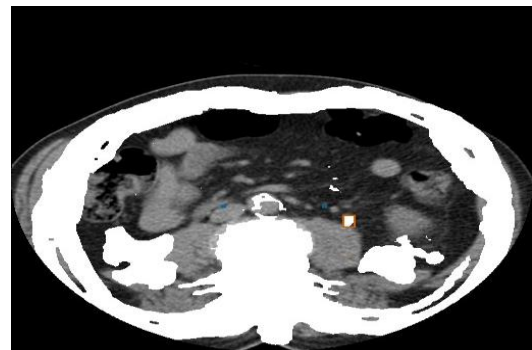


Figure 16. Patient number 2: Irregularly shaped abdomen.

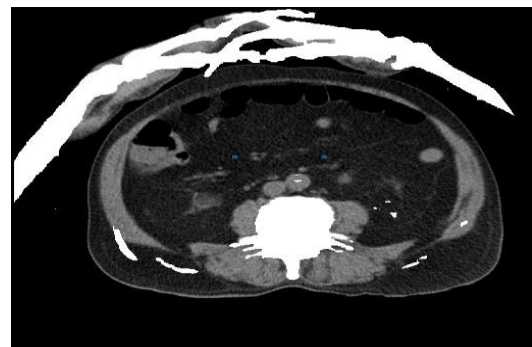


Figure 17. Patient number 3 shows the hands of the patient over the scanned image.

The program provided a contrary output because of the irregular height of the abdomen (inaccurate KUB scan of the torso). Program could not create a correct placement for arbitrary points which resulted to incorrect output. For Patient Number 3, The program provided an incorrect output for the patient due to inaccurate KUB scan of the torso; the patient placed his/her hand over the abdomen during the CT scan which prevented the program in creating the accurate placement for arbitrary points (Fig. 17).

In the case of Patient Number 25, the program was not able to detect the small stones that the physician identified. Threshold 120 was not able to provide a clear visual on the case, but calibration to threshold 85 provided a more distinct image of the diminutive kidney stone. The stone's size is 2mm, and the physician determined that this is a spatial case, opting not to include it in the patient's record. The researcher agreed that that the detection may be attributed noise (Fig. 18).

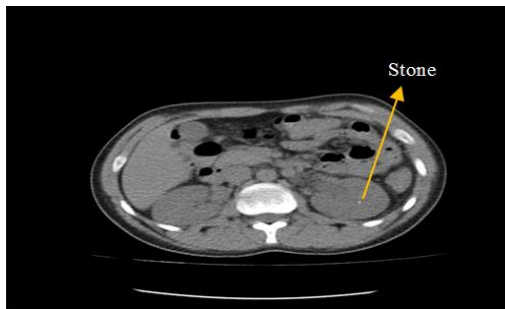


Figure 18. Patient number 25 have indistinct image of very small stones that was decided to be attributed to image noise.

For Patient Number 26, the program provided an incorrect output for the patient due to the location of the stone in the upper arbitrary point. Fig. 19 shows that the stone is not within the virtual enclosed region (spatial case). Lastly, for Patient Number 27, the program provided a flawed output from the proximity of the stone to the ribs (spatial case). In addition, some patients (e.g. Patient 21) for this study indicated diagnosis for 2 to 3 kidney stones, but closer examination using the program, determined that only one interconnected kidney stone was present. Further, the program provides more conclusive evidence to support diagnosis of small kidney stones. Small stones provide faint images in scans that may be overlooked even by seasoned physicians. Fig. 20 provides a sample in the study wherein the program was able to detect small stones that have was not indicated in the patient's record.

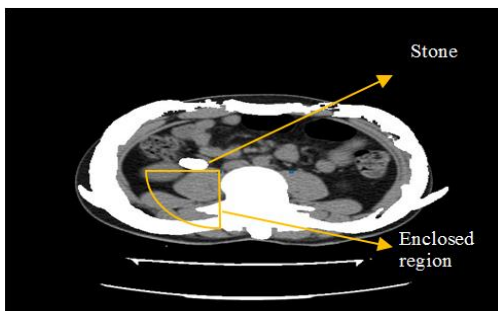


Figure 19. Patient number 26 displays a case of a stone outside the arbitrary point region.

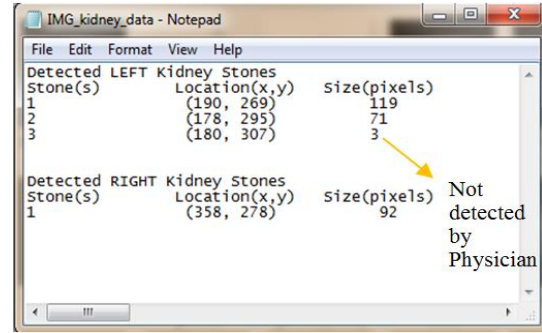


Figure 20. Sample case where a kidney stone not previously indicated in the patient's record was detected by the program.

C. Accuracy

The Confusion Matrix (Contingency Table) was used to compute for the accuracy of system. It is a prediction table that helped determines true positive, false positive, true negative and false negative results. Table III shows the program output and hospital record arranged in the Confusion Matrix. Accuracy was computed using the formula below:

TABLE III. PROGRAM OUTPUT AND HOSPITAL RECORD DIAGNOSIS DEMONSTRATED IN THE CONFUSION MATRIX

Prediction Outcome (program distinction)	ACTUAL VALUE (Physician's distinction)	
	24 cases true positive	1 case false positive
5 cases false negative	9 cases true negative	

$$TPR (true\ positive\ rate) = \frac{true\ positive}{true\ positive + false\ positive} = \frac{24}{24 + 1} = 0.96 = 96\% \quad (5)$$

$$FPR (false\ positive\ rate) = \frac{false\ positive}{false\ positive + true\ negative} = \frac{1}{1 + 9} = 0.071 = 7.14\% \quad (6)$$

$$ACCURACY = \frac{true\ positive + true\ negative}{total\ samples} = \frac{24 + 9}{39} = 33 \div 39 = 84.61\% \quad (7)$$

IV. CONCLUSIONS AND RECOMMENDATIONS

A. Conclusions

1) The semi-automated KUB CT image analysis prototype was developed to provide technical support in enhanced kidney stone detection. Its function to pinpoint the kidney area as region of interest, and kidney stones as objects of interests provide focused investigation for medical specialists.

2) The program's capacity to organize by sequence multiple KUB CT slices and combine these based on discernible images of the kidney allows the physician to evaluate an aggregate image from various images that the CT machine took for each patient. This provides cost-effective and timely delivery of diagnosis for both physician and patients.

3) The program's ability to detect and mark kidney stones and to identify stone size and location based on pixel values provide more efficient analysis of cases.

4) Its application in analyzing the cases of 39 kidney patients demonstrated high efficiency and high accuracy (84.61%).

5) It has demonstrated potential usefulness in kidney stone diagnosis and screening, however, the program is only a tool and the opinion of a qualified medical professional is required to validate its output.

B. Recommendations

1) For physicians and radiologists working on kidney stone detection – To ensure KUB CT images of patients are quality images by discerning that patients are properly positioned in the machine during medical examinations.

2) For future research – To (1) explore the accuracy and efficiency of the program in KUB CT scan images that use intravenous pyelogram (IVP) on patients. Since this type of method is also popular but not included in the analysis of the program, and (2) to explore enhanced segmentation of the kidney region to further improve accuracy in kidney stones detection.

ACKNOWLEDGMENT

The authors gratefully acknowledge the support and assistance provided by the Imam Reza Hospital in Iran in the development and application of the program prototype.

REFERENCES

- [1] F. L. Coe, A. Evan, and E. Worcester, "Kidney stone disease," *Journal of Clinical Investigation*, vol. 115, no. 10, pp. 2598-2608, 2005.
- [2] F. Grases, A. Costa-Bauza, and R. M. Prieto, "Renal lithiasis and nutrition," *Nutrition Journal*, vol. 5, no. 23, pp. 1-7, 2006.
- [3] V. Romero, H. Akpinar, and D. G. Assimos, "Kidney stones: A global picture of prevalence, incidence, and associated risk factors," *Reviews in Urology*, vol. 12, no. 2-3, pp. 86-96, 2010.
- [4] HPCS, *Scanning Systems, Computed Tomography, Full-Body*, Healthcare Product Comparison System (HPCS), ECRI Institute, Aug. 2002.
- [5] V. Chan and A. Perlas, "Basics of ultrasound imaging," in *Atlas of Ultrasound-Guided Procedures in Interventional Pain Management*, Springer New York, 2011, pp. 13-19.
- [6] S. Asadi, H. Hassanpour, and A. Pouyan, "Texture based image enhancement using gamma correction," *Middle-East Journal of Scientific Research*, vol. 6, no. 6, pp. 569-574, 2010.
- [7] R. C. Gonzalez and R. E. Woods, *Digital Image Processing*, 2nd ed., 1992, ch. 2, pp. 47-51 and ch. 10, pp. 568-611.

- [8] V. Caselles, F. Catta, T. Coll, and F. Dibos, "A geometric model for active contours in image processing," *Numerische Mathematik*, vol. 66, no. 1, pp. 1-31, 1993.
- [9] R. Malladi, J. A. Sethian, and B. C. Vemuri, "Shape modelling with propagation," *A Level Set Approach. Trans. of Pattern Analysis and Machine Intelligence*, vol. 17, no. 2, pp. 158-175, Feb. 1995.
- [10] A. Rosenfeld and A. C. Kak, *Digital Picture Processing*, 2nd ed., Academic Press, 1982, ch. 10.
- [11] E. R. Davies, *Machine Vision: Theory, Algorithms and Practicalities*, 4th ed., Academic Press, 1990, ch. 2, pp. 18-37 and ch. 4, pp. 83-97.
- [12] D. Vernon, *Machine Vision. Automated Visual Inspection and Robot Vision*, Prentice-Hall, 1991, ch. 4, pp. 49-50 and ch. 5, pp. 86-90.
- [13] J. Serra, *Image Analysis and Mathematical Morphology*, London: Academic Press, 1982, ch. 1, pp. 3-20 and ch. 2, pp. 50-59.
- [14] L. Shapiro and G. Stockman, *Computer Vision*, 1st ed., Prentice Hall, Jan. 2001, ch. 3, pp. 63-97.
- [15] R. Szeliski, *Computer Vision: Algorithms and Applications*, Springer, Sep. 2010, ch. 3, pp. 122-132.
- [16] A. Ruina and R. Pratap, *Introduction to Statics and Dynamics*, Oxford University Press, 2002, ch. 2, pp. 71-85 and ch. 3, pp. 138-152.
- [17] J. Kolomaznik, "Fast segmentation of kidneys in CT images," presented at the WDS '10 Proceedings of Contributed Papers, 2010, Part I, pp. 70-75.
- [18] D. Y. Kim and J. W. Park, "Computer-Aided detection of kidney tumor on abdominal computed tomography scans," *Acta Radiologica*, vol. 45, no. 7, pp. 791-795, 2004.
- [19] D. T. Lin, C. C. Lei, and S. W. Hung, "Computer-Aided kidney segmentation on abdominal CT images," *IEEE Trans. on Information Technology in Biomedicine*, vol. 10, no. 1, pp. 59-65, Jan. 2006.



Computer Science and minor in Information Technology. He is proud to be an alumnus of UPLB.



Vladimir Y. Mariano is an Associate Professor at Institute of Computer Science, University of the Philippines Los Baños.